Skeletal Radiol (2009) 38:51–59
DOI 10.1007/s00256-008-0577-6

SCIENTIFIC ARTICLE

Diffusion tensor imaging and fiber tractography of the median nerve at 1.5T: optimization of *b* value

Gustav Andreisek · Lawrence M. White · Andrea Kassner · George Tomlinson · Marshall S. Sussman

Received: 4 June 2008 / Revised: 28 July 2008 / Accepted: 3 August 2008 / Published online: 5 September 2008

Abstract
Objective The objective of this study was to systematically assess the optimal *b* value for diffusion tensor imaging and fiber tractography of the median nerve at 1.5 T.
Materials and methods This is a prospective study which was carried out with institutional review board approval and written informed consent from the study subjects. Fifteen healthy volunteers (seven men, eight women; mean age, 31.2 years) underwent diffusion tensor imaging of the wrist. A single-shot spin-echo-based echo-planar imaging sequence (TR/TE, 7000/103 ms) was performed in each subject at eight different *b* values ranging from 325 to 1,550 s/mm^2. Number and length of reconstructed fiber tracts, fiber density index (FDi), fractional anisotropy (FA), and apparent diffusion coefficient (ADC) were calculated for the median nerve. Signal-to-noise ratio (SNR) was also calculated for each acquisition. The overall image quality was assessed by two readers in consensus by ranking representative fiber tract images for each subject using a scale range from 1 to 8 (1 = best to 8 = worst image quality).
Results Longest fibers were observed for *b* values between 675 and 1,025 s/mm^2. Maximum FDi was found at *b* values of 1,025 s/mm^2. FA was between 0.5 and 0.6 for all *b* values. ADC gradually decreased from 1.44×10^{-3} to 0.92×10^{-3} mm^2/s with increasing *b* values. Maximum SNR± standard deviation (175.4±72.6) was observed at the lowest *b* value and decreased with increasing *b* values. SNR at *b* values of 1,025 s/mm^2 was 48.5% of the maximum SNR. Optimal fiber tract image quality was found for *b* values of 1,025 s/mm^2.
Conclusions The optimal *b* value for diffusion tensor imaging and fiber tractography of the median nerve at 1.5 T was 1,025 s/mm^2.

G. Andreisek · L. M. White
Division of Musculoskeletal Imaging,
Department of Medical Imaging,
Mount Sinai Hospital and the University Health Network,
University of Toronto,
600 University Ave,
Toronto, Ontario, Canada M5G 1X5

L. M. White
e-mail: lwhite@mtsinai.on.ca

A. Kassner
Department of Medical Imaging,
University Health Network, University of Toronto,
180 Dundas Street, 4th Floor, Suite 430, Room 428,
Toronto, Canada M5G 1X5
e-mail: andrea.kassner@utoronto.ca

G. Tomlinson
Division of Clinical Decision-Making & Health Care,
Department of Public Health Sciences, University of Toronto,
Toronto General Hospital,
Eaton North Wing, 13th Floor, Rm 13EN238, 200 Elizabeth St.,
Toronto, Ontario, Canada M5G 2C4
e-mail: george.tomlinson@utoronto.ca

M. S. Sussman
Department of Medical Imaging,
Toronto General Hospital, University of Toronto,
585 University Ave., NCSB 1C-572,
Toronto, Canada M5G 1X5
e-mail: marshall.sussman@utoronto.ca

Present address:
G. Andreisek (✉)
Institute of Diagnostic Radiology, University Hospital Zürich,
Rämistrasse 100,
CH-8091 Zürich, Switzerland
e-mail: gustav@andreisek.de

Keywords MRI · Diffusion tensor imaging · Fiber tractography · Median nerve

Introduction

Recently, several pilot studies with regard to the application of diffusion tensor imaging (DTI) and fiber tractography to peripheral nerves, e.g., the median, radial, and ulnar nerve at the wrist, the peroneal and tibial nerve at the knee/calf/ankle, as well as the sciatic nerve, have been published [1–6]. Possible clinical applications include the evaluation of peripheral nerves in compressive neuropathies such as the carpal tunnel syndrome or tracking of peripheral nerves in the presence of malignant neoplasm.

DTI is an emerging magnetic resonance (MR) imaging method and provides insight into tissue microstructure by monitoring random movement of water molecules which is usually restricted in anisotropic tissues [7]. Typically, diffusion tensor images show signal attenuation in the direction of a magnetic field gradient applied along a distinct direction in the three-dimensional space. The degree of signal attenuation is proportional to the water diffusivity [8, 9]. This diffusion data can either be used for determination of quantitative diffusion metrics such as apparent diffusion coefficient (ADC; value mathematically given by the average of the trace of the diffusion tensor) or fractional anisotropy (FA; quantitative index used to characterize the degree of diffusion anisotropy), or fiber tractography which is a method to visualize the DTI data. Fiber tractography is, most commonly, based on a line propagation technique in which a tracking line is propagated from a start point (seed) along the principal diffusion direction [10, 11]. It provides the capability to track individual nerves or nerve bundles and to display them on color-coded three-dimensional images.

In contrary to the central nervous system however, where DTI and fiber tractography are well-established techniques, its utility in the peripheral nervous system is challenging most likely due to the less water proton density of most tissues [2, 5]. In general, a diffusion-weighted pulse sequence should be highly sensitive to the degree of water molecular diffusion of the specific tissue to be imaged. In addition, an optimal balance between diffusion weighting and other imaging requisites, e.g., high signal-to-noise ratio, needs to be determined for each anatomic region in order to allow optimal image quality, and fiber tracking as well as anisotropic fiber characterization.

The primary parameter which determines sensitivity in a diffusion-weighted sequence is described by its *b* value, which is a user-prescribed parameter that is proportional to the amplitude and duration of the diffusion-sensitizing gradients [11–14]. Increasing *b* values reflect increasing diffusion weighting of a DTI acquisition [8]. In the aforementioned pilot studies, a wide range of *b* values (from 400 to 1,000 s/mm^2) were used in combination with single-shot spin-echo (ssSE)-based echo-planar imaging (EPI) pulse sequences to image structures of the peripheral nervous system [1, 3–6]. However, none of these studies clearly stated how optimal *b* values for imaging were chosen or determined. To the best of our knowledge, there is also no other published study in which the optimal *b* value for DTI and fiber tractography of peripheral nerves has been systematically assessed.

The purpose of this study was to systematically assess the optimal *b* value for DTI and fiber tractography of the median nerve at 1.5 T.

Materials and methods

Study subjects

This is a prospective cross-sectional study which was approved by the institutional research ethical board. Written informed consent was prospectively obtained from all study subjects.

Between January and March 2008, 15 healthy volunteers (seven men, eight women; mean/median age, 31.21/31.20 years; age range, 22–44 years) were prospectively included in this study. Inclusion criterion was age >18. Exclusion criteria were general contraindications for MRI (e.g. pacemaker), pregnancy, and history of prior surgery, cardiovascular, pulmonary, endocrine, metabolic, neurological, neuromuscular, or musculoskeletal disorders, respectively. All subjects were right-handed. Seven subjects (two men, five women; mean/median age, 28.7/28.6 years; age range, 22–34 years) underwent MRI of the left wrist, and eight subjects (five men, three women; mean/median age, 33.4/32.4 years; age range, 28–44 years) underwent MRI of the right wrist.

MR imaging

All MR imaging was performed on a 1.5-T MR scanner (Signa Excite HD, GE Healthcare, Waukesha, WI, USA) equipped with high-performance gradients (amplitude, 40 mT/m; slew rate, 200 T m^{-1} s^{-1}). An eight-channel transmit–receive wrist coil (Invivo, Orlando, FL, USA) was used. DTI acquisition of the wrist consisted of transaxial ssSE EPI sequences [TR/TE, 7000/103 ms; matrix size, 64×64; field of view (FoV), 120×120 mm; slice thickness, 4 mm, number of slices, 22; number of excitations (NEX), 2, acquisition time, 6:18 min]. Twenty-five diffusion-weighted direction-encoding images (b_{DWI}) and one single reference image without any diffusion weighting (b_0) were acquired. A total of eight DTI scans were performed in each subject with a range of *b* values: 325, 500, 675, 850, 1025,

1200, 1275, and 1550 s/mm^2. Slice location and all other image parameters were kept identical.

In addition to the DTI sequences, anatomic reference images were acquired by performing a standard transaxial T2-weighted fast spin-echo sequence (TR/TE, 3500/87 ms; echo train length, 11; matrix size, 256×224; FoV, 120×120 mm; slice thickness, 4 mm; number of slices, 22; NEX, 2; acquisition time, 4:26 min) in identical slice location as the ssSE EPI sequences. All imaging was performed in prone position with the hand extended over the head ("superman" position).

Post-processing including fiber tractography

For fiber tractography, images were transferred to a independent workstation and post-processed using dedicated DTI software (dtiStudio, release 2.4, John Hopkins University, Baltimore, MD, USA) by one single author (G.A., 7 years experience in MR imaging research). Mean b_{DWI} images (mean of all directions with same *b* value), FA, ADC and color-coded diffusion maps were calculated. A detailed description of these procedures and the software routines used for these calculations has been previously published [11]. Fiber tractography was performed by choosing an initial seed region of interest (ROI) at the level of the flexor retinaculum containing the nerve fibers of interest (Fig. 1). A free-hand ROI was chosen rather than round or oval ROIs since free-hand ROIs can be placed more precisely especially when the median nerve is interposed between tendons and does not have a round or oval cross-sectional area. The ROIs were minimally larger than the cross-sectional area of the median nerve in order to include all nerve fibers. Care was taken not to include surrounding anatomic structures (e.g., vessels or tendons). To select the ROIs, the median nerve was identified from the standard anatomic reference MR images, the mean b_{DWI} images, and the color-coded diffusion maps. The location of the ROIs was kept identical for the different *b* value acquisitions [5]. Tracking of fibers automatically started when the FA values of the voxels was above a threshold of 0.15 and was terminated at a threshold value of 0.35 or if the fiber angulation exceeded more than 55°. Similar reconstruction parameters were used in previous studies [1, 6].

Reconstructed fiber tract images were correlated with the anatomic images to confirm that reconstructed fibers did not exceed the anatomic boundaries of the nerve; otherwise, fiber tractography was repeated. Representative fiber tract images were saved (Fig. 2).

Quantitative analysis

Quantitative analysis was performed by the same author who post-processed the DTI datasets.

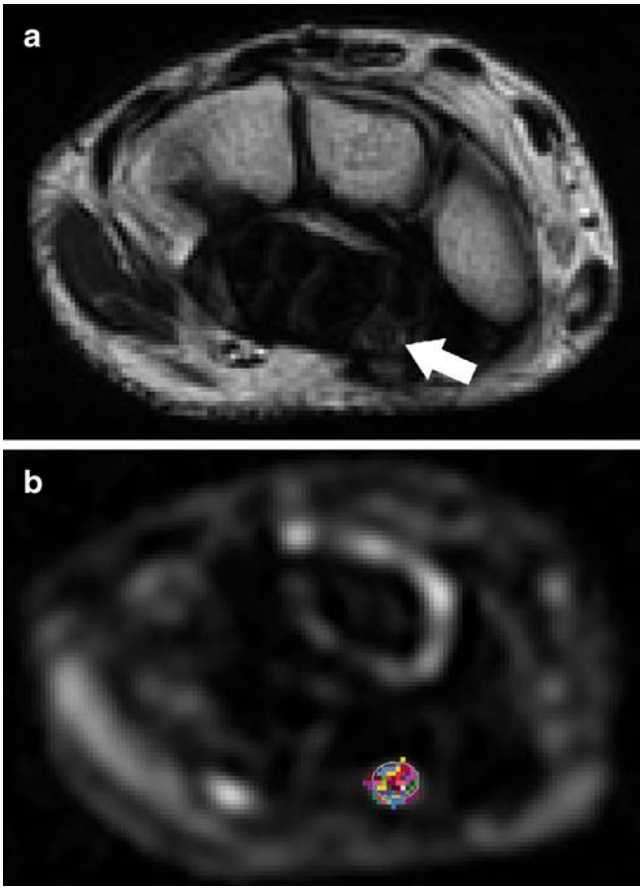

Fig. 1 **a** Transaxial T2-weighted fast spin-echo sequence (TR/TE, 3500/87 ms; echo train length, 11) of the left wrist at the level of the flexor retinaculum in a 28-year-old healthy female volunteer acquired as anatomic reference image to identify the median nerve (*arrow*). **b** Corresponding mean diffusion-weighted image (mean b_{DWI}) calculated from the diffusion-tensor imaging dataset acquired at a *b* value of 1,025 s/mm^2 in the same subject shows seed region-of-interest (*ROI*) for fiber tractography and automatically reconstructed color-coded fiber tracts within the ROI

Number and length of fibers, fiber density index, FA, and ADC

The number of fibers tracked throughout the seed ROI as used for tracking as well as their mean/maximum/minimum length (in mm) was evaluated within the DTI software. In addition, three quantities were determined: The fiber density index (FDi), which is a recently introduced quantitative index [15] which describes the density of fibers within a nerve bundle passing through a ROI, was calculated by dividing the number of fibers traversing an individual ROI by the area size of the ROI (in pixels). FA and ADC were calculated from new ROIs which were placed in the center of the nerves at the level of the flexor retinaculum [1]. To avoid partial volume artifacts, these ROIs were slightly smaller than the cross-sectional area of the median nerve. The size of the ROIs depended on the cross-sectional area of the nerve. All ROIs were placed in one slice only.

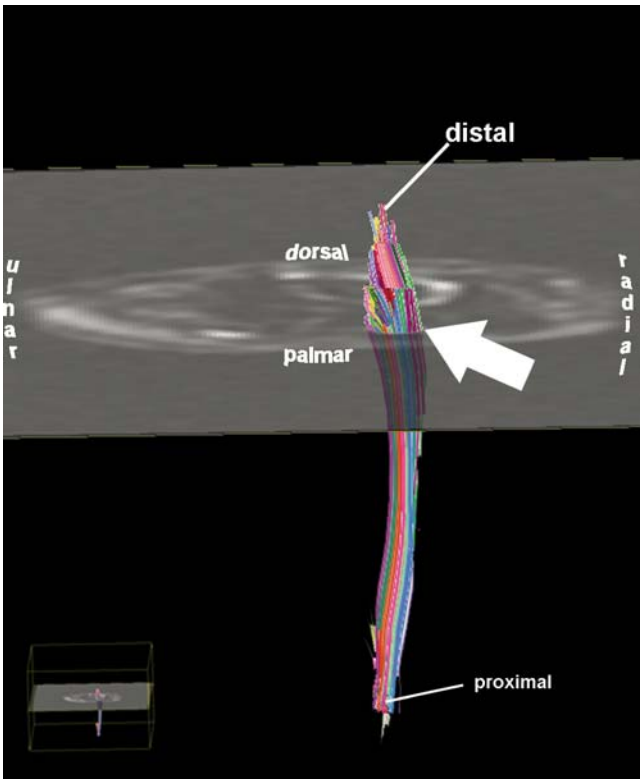

Fig. 2 Representative three-dimensional fiber tract image created from the same data set as in Fig. 1 shows reconstructed color-coded fiber tracts passing through the seed ROI (*arrow*); oblique trans-axial view from palmar to dorsal. Mean length of tracked fibers was 31.5 mm (range, 8.1–71.5 mm), fiber density index was 42.5

Signal-to-noise ratio

To calculate signal-to-noise ratio (SNR), the mean signal intensity (SI) was determined for all mean b_{DWI} and b_0 images. For the determination of the SI of the nerve, the same ROIs as used for FA and ADC calculations were used. The background noise was calculated from the standard deviation (SD) of a ROI (size, 2 cm^2) placed outside of the wrist. The SNR was then calculated using the following equation:

$$\mathrm{SNR} = \frac{SI_{\mathrm{Nerve}}}{SD_{\mathrm{Background\_noise}}} \times \left(\sqrt{2 - \frac{\pi}{2}}\right).$$

The equation included a correction factor (square root of $2-\pi/2$) which was used to account for the systemic error in signal measurements in magnitude images [16, 17].

In addition, in a randomly chosen subset of six subjects, the SNR of each single diffusion-weighted direction-encoded and reference MR images (b_0) was determined for each of the eight DTI acquisitions.

Qualitative image analysis

For each subject, a set of eight fiber tract images was shown to two experienced readers [one radiologist (L.M. W.) with 15 years experience in musculoskeletal MR imaging; one physicist (M.S.S.) with 6 years experience in MR imaging research, respectively]. Each image of the set was acquired at a different *b* value. Image sets were presented in a randomly selected order. Both readers were blinded to the corresponding *b* values and the personal data of the subject. Both readers were ask to rank, in consensus, the image quality based upon a qualitative evaluation of fiber tract order and homogeneity, fiber tract organization, fiber length, appearance of fiber bundles in boundary regions, and apparent density of fiber bundles. Image quality was ranked using an eight-point rank scale (from 1 = best to 8 = worst).

Statistical analysis

All computations were performed by one author (G.A.) using Excel® (release 12.0.6., Microsoft, Redmond, WA, USA) and SPSS® (release 12.0.1, SPSS Inc., Chicago, IL, USA).

FDi and SNR values as well as ranking results for qualitative image analysis were summarized using bar charts with error bars to show the structure of the original raw data (i.e., means and 95% confidence interval of means) and the differences of means between different *b* values [18].

To assess the true variability in the mean fiber length, FDi, and FA across the eight *b* values, the parametric bootstrap method was used [19, 20]. Therefore, 10,000 replicate datasets were generated with the same mean and variance structure as the DTI datasets in our sample of 15 subjects. For each replicate dataset, the mean outcome (fiber length, FDi, or FA) for each *b* value was obtained, and *b* values were ranked best to worst by their means. Across the 10,000 replicate datasets, the percentage of times that each *b* value was best, second best,…, worst was tabulated. This percentage can be interpreted as the probability that a particular *b* value has the corresponding rank order.

Qualitative data were tested using a randomization test to test whether the observed rakings of fiber tract image quality indicated a real preference for a particular *b* value. The null hypothesis for this was that the quality rankings are random. This would mean that for any given subject, there was an equal chance that each of the *b* values could be first, second, etc., and that no *b* value was preferred to any other.

Results

Length of fibers, fiber density index, FA, and ADC

Fiber tract images were produced for all *b* values (Fig. 3). In three of 15 subjects (20%), fiber tractography was

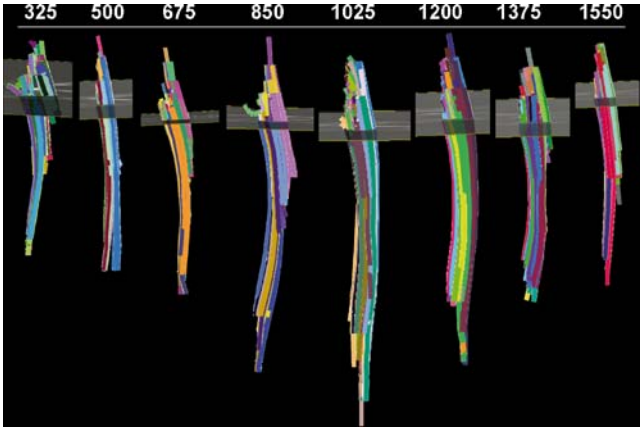

Fig. 3 Image shows a set of eight fiber tract images which were acquired at *b* values ranging from 325 to 1,500 s/mm^2 (*numbers on the top* indicate *b* value). Images were reconstructed from the diffusion tensor imaging (*DTI*) dataset of the same subject as in Figs. 1 and 2. Longest fibers are observed at *b* values of 1,025 s/mm^2

repeated since initial reconstructed fibers exceeded the anatomic boundaries of the median nerve.

The longest fibers were observed for MR sequences acquired with *b* values of 675, 850, and 1,025 s/mm^2 (Table 1). Using the bootstrap method with 10,000 replicate datasets, the probabilities for these *b* values having the longest fibers were found to be 41.4%, 35.1%, and 14.5%, respectively. Shorter fibers were seen at very low (325 s/mm^2) and very high (1,375 and 1,550 s/mm^2) *b* values (Table 1). The probabilities across the replicate datasets for these *b* values having the shortest fibers were 45.2%, 24.6%, and 24.7%, respectively.

The highest densities of tracked fibers per ROI (=FDi) were observed at *b* values of 1,025 s/mm^2 (Fig. 4a). At this *b* value, 97.3% of the 10,000 replicate datasets had the highest mean FDi value (Fig. 4b). This represents a 97.3% probability of *b* values of 1,025 s/mm^2 having the highest FDi. Observed fiber densities per ROI were lower for all *b* values other than *b*=1,025 s/mm^2, and their probabilities across the replicate datasets of having a higher fiber density index than *b*=1,025 s/mm^2 were under 2.6%.

The mean observed FA was between 0.5 and 0.6 with FA measurements showing a consistently low standard deviation (range, 0.1 to 0.2). Probability calculations across replicate datasets showed no evidence for differences between FA of different *b* values. The ADC gradually decreased from 1.44×10^{-3} mm^2/s for *b* values of 325 s/mm^2 to 0.92×10^{-3} mm^2/s for *b* values of 1,550 s/mm^2.

Signal-to-noise ratio

Maximum SNR (mean±SD, 114.9±47.6) for mean diffusion-weighted direction-encoding MR images (mean b_{DWI} images) was observed at the lowest *b* value (325 s/mm^2). The mean SNR decreased with increasing *b* values (Fig. 5). SNR for a *b* value of 1,025 s/mm^2 was 55.7±20.6, which corresponds to (55.7/114.9)×100=48.5% of the maximum SNR. SNR calculated from the mean reference images without diffusion weighting (mean b_0 images) acquired at *b* values of 325, 500, 675, 850, 1,025, 1,200, 1,375, and 1,550 s/mm^2 was 39.6±12.6, 35.5±15.3, 37.7±13.2, 38.4±12.6, 38.1±11.7, 38.2±10.2, 36.9±14.0, and 39.4±11.4 (mean±SD), respectively.

The SNR calculation for each individual diffusion-weighted MR image of each of the eight MR sequences in a subset of six subjects showed a uniform pattern of SNR across all 25 direction-encoding MR images. This pattern was similar for all *b* values.

Quality of fiber tract images

Fiber tract images acquired with a *b* value of 1,025 s/mm^2 were either ranked as 1 (best image quality in seven

Table 1 DTI of the median nerve at the level of the flexor retinaculum: number of tracked fibers, fiber length, fiber density indices, fractional anisotropy, and apparent diffusion coefficients (*n*=15)

b value (s/mm^2)	No. of fibers (mean±SD)	Fiber length (mm)			FDi	FA	ADC ($\times10^{-3}$, mm^2/s)
		Mean±SD	Min±SD	Max±SD	Mean±SD	Mean±SD	Mean±SD
325	120.6±39.8	13.5±2.1	5.0±2.3	24.3±4.9	10.8±3.8	0.5±0.1	1.44±0.19
500	129.8±65.7	15.1±3.2	6.9±1.5	25.5±7.8	17.6±4.8	0.6±0.1	1.36±0.18
675	114.8±32.8	16.1±4.1	10.6±6.9	25.8±9.1	21.3±6.0	0.5±0.2	1.27±0.15
850	100.7±34.9	16.1±4.4	7.3±3.7	26.5±6.9	26.1±7.5	0.5±0.2	1.19±0.16
1,025	86.7±36.5	15.7±5.3	7.3±3.3	25.0±6.7	30.5±8.0	0.5±0.2	1.11±0.13
1,200	89.1±39.7	15.0±6.1	9.0±3.5	22.4±8.7	28.2±9.3	0.6±0.1	1.05±0.14
1,375	99.3±29.2	13.7±3.2	7.2±2.4	23.3±7.5	21.0±7.7	0.6±0.1	0.95±0.15
1,550	93.3±40.4	13.9±4.7	7.3±2.8	19.5±7.7	17.7±5.4	0.5±0.1	0.92±0.11

No. number, *SD* standard deviation, *Min* minimum, *Max* maximum, *FDi* fiber density index, *FA* fractional anisotropy, *ADC* apparent diffusion coefficient ($\times10^{-3}$ mm^2/s)

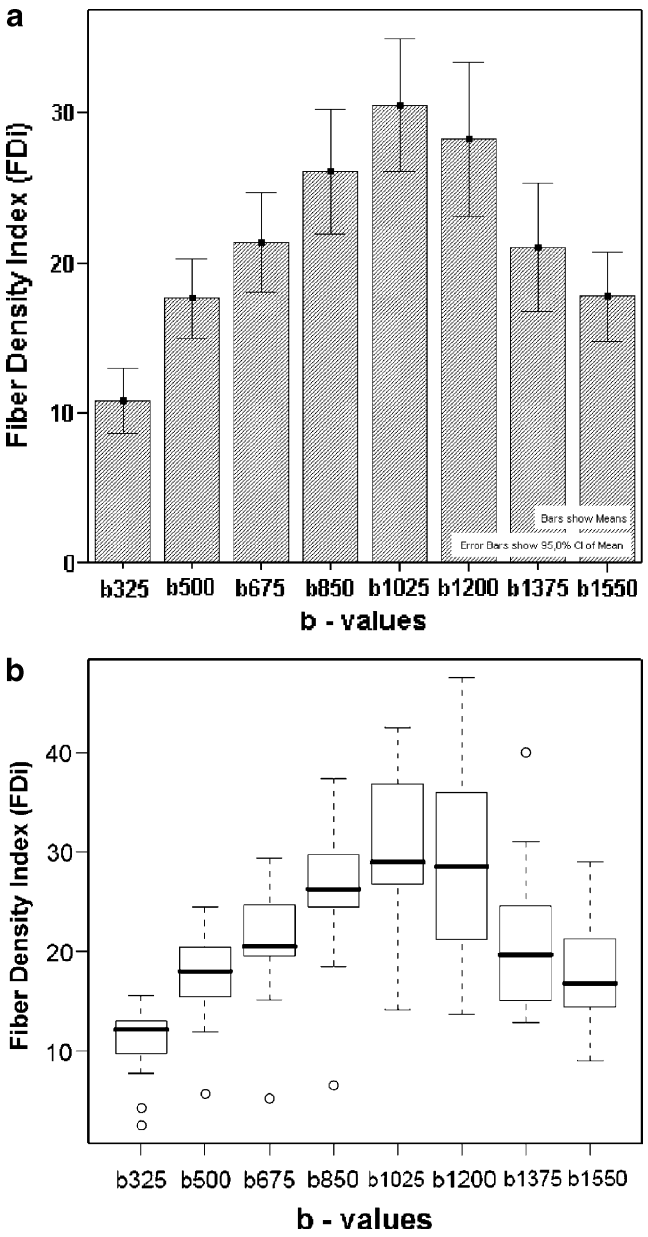

Fig. 4 **a** Diagram shows observed fiber density indices (*FDi*) for diffusion tensor images acquired at eight different *b* values. *Bars* represent mean density of tracked fibers (FDi) calculated as number of fibers passing the seed ROI divided by the size of the seed ROI. *Error bars* show 95% confidence interval (*CI*) of means. **b** *Box plots* show calculated fiber density indices (*FDi*) across 10,000 replicate datasets using the parametric bootstrap

subjects), 2 (second best image quality in three subjects) or 3 (third best image quality in four subjects; Table 2). In only one subject, their image quality was ranked lower than that, namely 4 (fourth best image quality). This resulted in the best rank for image quality across all *b* values (Fig. 6). Considering our null hypothesis (see "Statistical analysis"), we performed a randomization test to calculate the chance that any *b* value will receive seven or more first place rankings. The chance was 0.9% (p=0.009).

Discussion

There is a growing interest among researchers and radiologists in the use of MR imaging techniques such as DTI and fiber tractography for imaging the musculoskeletal system [1–6, 21–26]. In our study, we acquired a series of identical single-shot spin-echo-based echo-planar imaging MR sequences in a cohort of 15 healthy volunteers in order to assess the optimal imaging parameters, i.e., the optimal *b* value, for DTI and fiber tractography of peripheral nerves at 1.5 T.

Using low *b* values of 325 s/mm^2, the fiber tracking reconstruction algorithm in our study was not stable, and reconstructed fiber tracts were relatively unorganized and tracking length was short. This likely reflects the limited sensitivity of such low *b* value acquisitions to molecular diffusion within the median nerve. Fiber tracts were also short when high *b* values, i.e., 1,375 and 1,550 s/mm^2 were used. This may be explained by the fact that with increasing diffusion weighting, the SNR decreases [27, 28], while fiber tracking algorithms are additionally sensitive to lower SNR acquisitions [28]. Low SNR leads to an increased number of voxels with a signal intensity magnitude below the user-prescribed noise cutoff value which is used by the DTI software to select voxels for fiber tracking. This may lead to premature termination of the reconstructed fibers [29]. In our study, we used the bootstrap method rather than statistical tests which would simply compare the actual

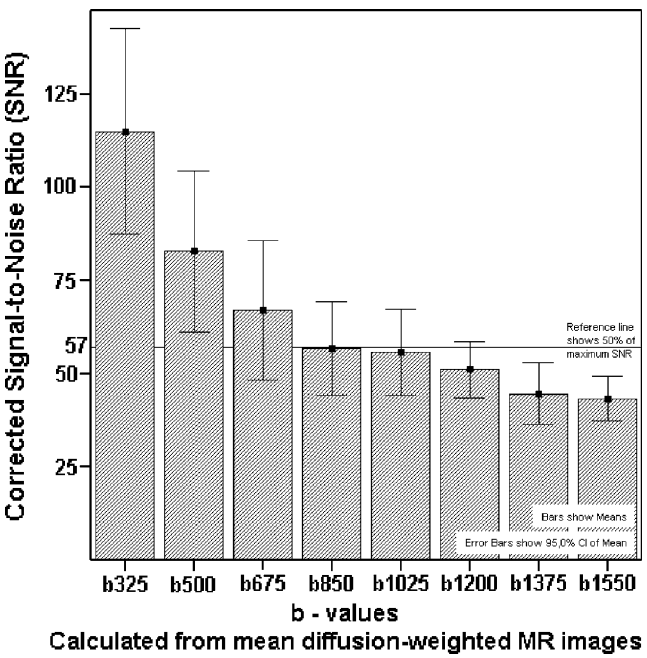

Fig. 5 Diagram shows signal-to-noise ratio (*SNR*) for diffusion tensor images acquired at eight different *b* values. *Bars* represent mean SNR calculated from mean diffusion-weighted images (b_{DWI}). *Error bars* show 95% confidence interval (*CI*) of means. Please note the decrease of SNR with increasing *b* values

Table 2 Fiber tractography of the median nerve: assessment (ranking) of fiber tract image quality

Subject no.	*b* value							
	b325	b500	b675	b850	b1025	b1200	b1375	b1550
1	8	7	6	5	3	2	1	4
2	7	6	8	5	1	4	3	2
3	8	6	3	7	1	4	2	5
4	8	7	6	2	3	4	5	1
5	8	2	6	7	3	1	5	4
6	8	7	6	5	2	3	1	4
7	8	4	5	7	1	2	6	3
8	8	5	7	3	2	1	6	4
9	8	7	4	5	1	3	6	2
10	8	2	4	7	1	3	5	6
11	8	6	5	4	1	7	3	2
12	7	4	1	6	3	2	5	8
13	8	7	6	1	4	2	3	5
14	7	8	2	6	1	5	4	3
15	8	7	3	1	2	4	5	8
Mean of 1/Rank	0.13	0.21	0.28	0.32	0.67	0.42	0.35	0.33

Both readers ranked, in consensus, images by their quality from 1 = best image quality to 8 = worst image quality.

mean fiber length at different *b* values to assess which *b* value would be best to produce the longest fibers during fiber tractography. The bootstrap method was based on the generation of 10,000 replicate (virtual) datasets with the same mean and variance structure as the DTI datasets in our sample of 15 subjects. Using this statistical approach, we found that with a probability of 41.4%, the longest fibers will be seen when DTI dataset acquired at *b* values of 675 s/mm^2 are used for the post-processing.

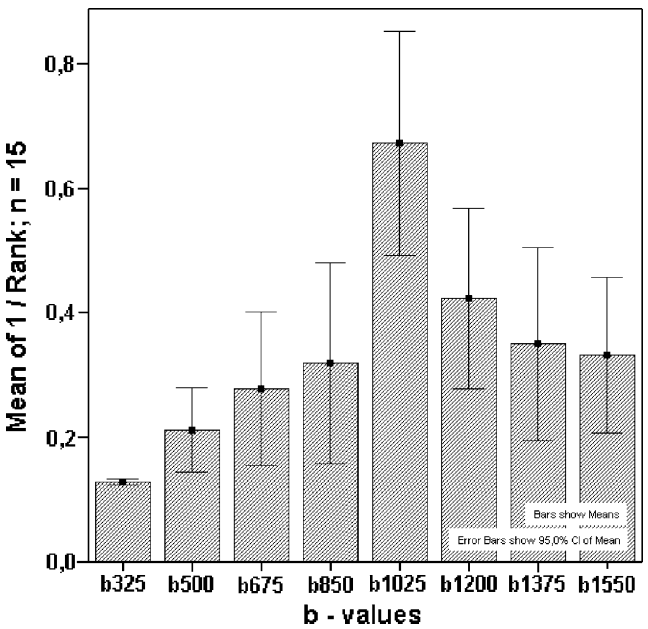

Fig. 6 Diagram shows image quality of representative fiber tract images acquired at eight different *b* values as assessed by two blinded readers in consensus. Images were ranked from 1 = best image quality to 8 = worst image quality (for raw data please refer to Table 2). *Bars* represent the mean rank which was assigned to the each image. For display purposes, the quotient 1/rank was calculated and assigned to the *y*-axis of the diagram

In our study, we calculated the FDi to describe the density of discernable continuous fibers tracts passing through a ROI which was placed in the median nerve at the level of the flexor retinaculum. The FDi was originally used in the brain to describe the density of white matter fibers within a bundle passing through a single pixel or a ROI. It depends on imaging parameters and fiber tract reconstruction factors such as spatial resolution, FA cutoff value, and fiber angulation threshold [15]. Our statistical analysis (bootstrap method) showed that with 97.3% probability, FDi values will be highest at *b* values of 1,025 s/mm^2 rather than at other *b* values. To our knowledge, no previous study has reported FDi values for peripheral nerves.

We also studied FA. We found FA values ranging from 0.5±0.2 to 0.6±0.1. Our FA values are in perfect agreement with previously published data where the mean FA (±SD) of the median nerve were reported to be 0.6±0.1 at *b* values of 1,000 s/mm^2 [1, 4, 5]. Interestingly, we found in the literature that the FA value is not uniform across the course of the median nerve. FA measures at the level of the flexor retinaculum were reported to be significantly different from those measured at the level of the forearm or at the level of the distal radio-ulnar joint. Moreover, FA of the median nerve was found to decrease with increasing age of the subjects [1]. We did not perform an age-related sub-analysis of our FA data, since most of the subjects in our study cohort were quite young and within the same age range.

Our study is the first DTI study in peripheral nerves where the association of diffusion weighting and SNR was systematically assessed. In general, we observed decreasing SNRs with increasing *b* values. This observation is similar to observations made in diffusion-weighted MR imaging of the brain [2, 10, 12, 30]. SNR effects must be taken into account whenever metric data, such as ADC, are calculated from DTI images. In our study, the mean ADC at *b* values of 1,025 s/mm^2 was $1.11\pm0.13\times10^{-3}$ mm^2/s. This is in good agreement with previous data acquired at corresponding *b* values where ADC values between 0.97 ± 0.03 and $0.98\pm0.02\times10^{-3}$ mm^2/s were found for the median nerve [1]. With increasing *b* values, however, we found decreasing ADC values, an observation previously described as systematic error in the quantitative evaluation of diffusion-weighted imaging data [28, 31]. This error was found to be related to a varying SNR at different diffusion weightings and to cause systematically decreased ADC values at higher *b* values. Different theoretical models with regard to correction schemes for the underlying variation in SNR have recently been proposed which would allow exact determination of ADC in diffusion imaging studies [17, 31]. Neither of these models was applied in our study, however, as there is still discussion on their efficiency.

Within the range of *b* values used in our study, our results for fiber characteristics (i.e., FDi) and image quality suggest the use of a *b* value of 1,025 s/mm^2 for DTI and fiber tractography of the median nerve at 1.5 T utilizing a multi-channel wrist coil. The SNR at this *b* value was shown to be approximately 50% of the maximum SNR observed at the lowest *b* value of 325 s/mm^2. DTI in the clinics, however, is different from our experimental setting as usually, the echo times are not constant during DTI acquisitions. In typical DTI acquisitions, the minimum allowed TE is chosen to maximize SNR. SNR could further be improved by, e.g., using higher field strength, different coil technology [32], or by employing the individual coil sensitivities using sensitivity encoding techniques such as SENSE which could help to improve the image quality of single-shot echo-planar imaging by reducing the train of gradient echoes in combination with a faster k-space traversal per unit time [33]. However, under the condition of improved SNR, other *b* values might be optimal for DTI. Consequently, the evaluation of the optimal *b* value then needs to be repeated.

In addition, in some clinical settings, DTI may only be performed to visualize peripheral nerves by fiber tractography (e.g., to evaluate the course of a nerve in the presence of a neoplasm). In these cases where the determination of other fiber characteristics such as FDi may not be important, *b* values lower than 1,025 s/mm^2 might be used for data acquisition. Our results showed that reconstructed fiber tracts are expected to be longest at *b* values of 675 and 850 s/mm^2.

There are several limitations to the technique used in our study. In-plane resolution was 1.875×1.875 mm^2, which might be insufficient to image smaller peripheral nerves. DTI data processing is not standardized [7] and different fiber tracking software uses different fiber reconstruction algorithms [34]. In addition, we used the same parameters for fiber tracking as previous studies [1, 6]; however, there are no studies which have proven that these parameters are "optimal" for DTI and fiber tracking of peripheral nerves. Nevertheless, we do not expect that using other reconstruction parameters would change the overall results of our study. Another limitation is that no image co-registration was performed to minimize distortions and artifacts prior to image analysis. Inter- and intra-observer reliabilities for DTI and fiber tractography of the median nerve were also not evaluated in this study. However, this is the topic of a future study.

In conclusion, in our study, the optimal *b* value for DTI and fiber tractography of the median nerve at 1.5 T was 1,025 s/mm^2.

Disclosure statements Dr. Gustav Andreisek is supported by a grant from the Holcim Foundation for the Advancement of Scientific Research, Switzerland.

References

1. Kabakci N, Gurses B, Firat Z, Bayram A, Ulug AM, Kovanlikaya A, et al. Diffusion tensor imaging and tractography of median nerve: normative diffusion values. AJR Am J Roentgenol 2007; 189(4): 923–927.
2. Skorpil M, Engstrom M, Nordell A. Diffusion-direction-dependent imaging: a novel MRI approach for peripheral nerve imaging. Magn Reson Imaging 2007; 25(3): 406–411.
3. Tsuchiya K, Fujikawa A, Tateishi H, Nitatori T. Visualization of cervical nerve roots and their distal nerve fibers by diffusion-weighted scanning using parallel imaging. Acta Radiol 2006; 47 (6): 599–602.
4. Meek MF, Stenekes MW, Hoogduin HM, Nicolai JP. In vivo three-dimensional reconstruction of human median nerves by diffusion tensor imaging. Exp Neurol 2006; 198(2): 479–482.
5. Hiltunen J, Suortti T, Arvela S, Seppa M, Joensuu R, Hari R. Diffusion tensor imaging and tractography of distal peripheral nerves at 3 T. Clin Neurophysiol 2005; 116(10): 2315–2323.
6. Skorpil M, Karlsson M, Nordell A. Peripheral nerve diffusion tensor imaging. Magn Reson Imaging 2004; 22(5): 743–745.
7. Nucifora PG, Verma R, Lee SK, Melhem ER. Diffusion-tensor MR imaging and tractography: exploring brain microstructure and connectivity. Radiology 2007; 245(2): 367–384.
8. Mori S, Zhang J. Principles of diffusion tensor imaging and its applications to basic neuroscience research. Neuron 2006; 51(5): 527–539.
9. Landman BA, Farrell JA, Jones CK, Smith SA, Prince JL, Mori S. Effects of diffusion weighting schemes on the reproducibility of DTI-derived fractional anisotropy, mean diffusivity, and principal eigenvector measurements at 1.5 T. Neuroimage 2007; 36(4): 1123–1138.

10. Mori S, van Zijl PC. Fiber tracking: principles and strategies—a technical review. NMR Biomed 2002; 15(7–8): 468–480.
11. Jiang H, van Zijl PC, Kim J, Pearlson GD, Mori S. DtiStudio: resource program for diffusion tensor computation and fiber bundle tracking. Comput Methods Programs Biomed 2006; 81 (2): 106–116.
12. Lee SK, Kim DI, Kim J, Kim DJ, Kim HD, Kim DS, et al. Diffusion-tensor MR imaging and fiber tractography: a new method of describing aberrant fiber connections in developmental CNS anomalies. Radiographics 2005; 25(1): 53–65, discussion 66–58.
13. Mori S, Barker PB. Diffusion magnetic resonance imaging: its principle and applications. Anat Rec 1999; 257(3): 102–109.
14. Masutani Y, Aoki S, Abe O, Hayashi N, Otomo K. MR diffusion tensor imaging: recent advance and new techniques for diffusion tensor visualization. Eur J Radiol 2003; 46(1): 53–66.
15. Roberts TP, Liu F, Kassner A, Mori S, Guha A. Fiber density index correlates with reduced fractional anisotropy in white matter of patients with glioblastoma. AJNR Am J Neuroradiol 2005; 26 (9): 2183–2186.
16. Henkelman RM. Measurement of signal intensities in the presence of noise in MR images. Med Phys 1985; 12(2): 232–233.
17. Dietrich O, Heiland S, Sartor K. Noise correction for the exact determination of apparent diffusion coefficients at low SNR. Magn Reson Med 2001; 45(3): 448–453.
18. Applegate KE, Tello R, Ying J. Hypothesis testing III: counts and medians. Radiology 2003; 228(3): 603–608.
19. Efron B, Halloran E, Holmes S. Bootstrap confidence levels for phylogenetic trees. Proc Natl Acad Sci USA 1996; 93(23): 13429–13434.
20. Efron B, Tibshirani RJ. An introduction to the bootstrap. London, UK: Chapman & Hall; 1993.
21. Taoka T, Hirabayashi H, Nakagawa H, Sakamoto M, Myochin K, Hirohashi S, et al. Displacement of the facial nerve course by vestibular schwannoma: preoperative visualization using diffusion tensor tractography. J Magn Reson Imaging. 2006; 24(5): 1005–1010.
22. Rossi C, Boss A, Lindig TM, Martirosian P, Steidle G, Maetzler W, et al. Diffusion tensor imaging of the spinal cord at 1.5 and 3.0 Tesla. Rofo 2007; 179(3): 219–224.
23. Lansdown DA, Ding Z, Wadington M, Hornberger JL, Damon BM. Quantitative diffusion tensor MRI-based fiber tracking of human skeletal muscle. J Appl Physiol 2007; 103(2): 673–681.
24. Zaraiskaya T, Kumbhare D, Noseworthy MD. Diffusion tensor imaging in evaluation of human skeletal muscle injury. J Magn Reson Imaging 2006; 24(2): 402–408.
25. Damon BM, Ding Z, Anderson AW, Freyer AS, Gore JC. Validation of diffusion tensor MRI-based muscle fiber tracking. Magn Reson Med 2002; 48(1): 97–104.
26. Budzik JF, Le Thuc V, Demondion X, Morel M, Chechin D, Cotten A. In vivo MR tractography of thigh muscles using diffusion imaging: initial results. Eur Radiol 2007; 17(12): 3079–3085.
27. Huang H, Zhang J, van Zijl PC, Mori S. Analysis of noise effects on DTI-based tractography using the brute-force and multi-ROI approach. Magn Reson Med 2004; 52(3): 559–565.
28. Farrell JA, Landman BA, Jones CK, Smith SA, Prince JL, van Zijl PC, et al. Effects of signal-to-noise ratio on the accuracy and reproducibility of diffusion tensor imaging-derived fractional anisotropy, mean diffusivity, and principal eigenvector measurements at 1.5 T. J Magn Reson Imaging 2007; 26(3): 756–767.
29. Chen B, Hsu EW. Noise removal in magnetic resonance diffusion tensor imaging. Magn Reson Med 2005; 54(2): 393–401.
30. Bammer R, Acar B, Moseley ME. In vivo MR tractography using diffusion imaging. Eur J Radiol 2003; 45(3): 223–234.
31. Bastin ME, Armitage PA, Marshall I. A theoretical study of the effect of experimental noise on the measurement of anisotropy in diffusion imaging. Magn Reson Imaging 1998; 16(7): 773–785.
32. Gilbert G, Simard D, Beaudoin G. Impact of an improved combination of signals from array coils in diffusion tensor imaging. IEEE Trans Med Imaging 2007; 26(11): 1428–1436.
33. Jaermann T, Crelier G, Pruessmann KP, Golay X, Netsch T, van Muiswinkel AM, et al. SENSE-DTI at 3 T. Magn Reson Med 2004; 51(2): 230–236.
34. Staempfli P, Reischauer C, Jaermann T, Valavanis A, Kollias S, Boesiger P. Combining fMRI and DTI: A framework for exploring the limits of fMRI-guided DTI fiber tracking and for verifying DTI-based fiber tractography results. Neuroimage 2008; 39(1): 119–126.